



1 **A vertical transport window of water vapor in the troposphere**
2 **over the Tibetan Plateau with implication for global change**

3

4 **Xiangde Xu¹, Chan Sun^{1,2}, Deliang Chen³, Tianliang Zhao^{2*}, Jianjun Xu⁴, Shengjun**
5 **Zhang¹, Juan Li², Bin Chen¹, Yang Zhao¹, Lili Dong¹, Xiaoyun Sun², Yan Zhu²**

6

7 ¹ State Key Laboratory of Disastrous Weather, China Academy of Meteorological
8 Sciences, Beijing, 100081, China;

9 ² Collaborative Innovation Center for Meteorological Disaster Forecast, Warning and
10 Assessment, Nanjing University of Information Science and Technology, Nanjing
11 210044, China;

12 ³ Regional Climate Group, Department of Earth Sciences, University of Gothenburg,
13 Sweden;

14 ⁴ South China Sea Institute of Marine Meteorology, Guangdong Ocean University,
15 Zhanjiang 524088, China

16 * Corresponding author. **Email:** tlzhao@nuist.edu.cn

17

18

19

20



21 **Abstract**

22 By using the multi-source data of meteorology over recent decades, this study
23 discovered a summertime “hollow wet pool” in the troposphere with a center of high
24 water vapor over Asian water tower (AWT) on the Tibetan Plateau (TP), where is
25 featured by a vertical transport “window” in the troposphere. The water vapor transport
26 in the upper troposphere extends from the vertical transport window over the TP with the
27 significant connections among the Arctic, Antarctic and TP regions, highlighting an
28 effect of TP’s vertical transport window of tropospheric vapor in the “hollow wet pool”
29 on global change. The vertical transport window was built by the AWT’s thermal forcing
30 in associated with the dynamic effect of the TP’s “hollow heat island”. Our study
31 improve the understanding on the vapor transport over the TP with an important
32 implication to global change.

33



34

35 1. Introduction

36 The Tibetan Plateau (TP) is the largest high terrain in the world, known as "the roof
37 of the world" with an averaged altitude over 4,000 meters. The rivers, such as the
38 Yangtze River, Yellow River, Lancang River and Ganges River, are all originated from
39 the TP, which is regarded as the "Asian Water Tower" (AWT) (Xu et al., 2008). The
40 Three-River-Source (Yangtze, Yellow, and Lancang Rivers) region (TRSR) in the eastern
41 TP is the core area of the AWT (Xu et al., 2014). The observed "CISK-like mechanism"
42 is an important mechanism sustaining the atmospheric "water tower" over the AWT.
43 Connecting with the cloud and precipitation in the AWT, the plausible hydrological
44 cycles could be realized with the transport of water vapor from tropical oceans up to the
45 TP (Xu et al., 2014).

46

47 Water vapor plays an important role in global environment and climate changes
48 (Tian et al.,2009; Solomon et al.,2010). The ratio of strong convective clouds to total
49 clouds over the Tibetan Plateau (TP) is about 5 times to the global ratio, and the frequent
50 occurrences of strong convective clouds could be largely attributed to the TP's large
51 topography (Luo et al.,2011; Su et al.,2006). The water vapor in the tropical upper
52 troposphere is mainly originated from the tropical lower troposphere through convective
53 transport and evaporation of convectively transported or in situ produced cloud ices (Tian
54 et al.,2004; James, et al.,2008). Water vapor was first lifted by convection over the Bay
55 of Bengal and the South China Sea and then transported upwards the tropical tropopause
56 layer via the monsoon anticyclonic circulations towards Northwest India (Yanai, et al.,



57 1973; Chen, et al., 2012). TP is a moisture sink in summer, having a net moisture
58 convergence of 4 mm/day, where the convergence was enhanced from 1979 to 2018
59 (Feng and Zhou, 2012; Xu, et al., 2020). In general, Asian monsoon circulation provides
60 an effective pathway for regional water vapor transport to the TP (Wang, et al.,2017). An
61 important role of the anticyclone over the TP is verified in the exchange of water vapor
62 between the troposphere and stratosphere (Garny, et al., 2016; Fu, et al., 2006) . Many
63 studies have been focused on the transport of water vapor into upper troposphere and
64 lower stratosphere from the tropical oceans to the TP (Chen, et al., 2012; Wang, et
65 al.,2017; Xie, et al.,2018; Randel, et al.,2013) . However, not enough attention has been
66 paid to the vertical transport of water vapor in the troposphere over the TP.

67

68 The following questions are also of great concern in the TP' vertical transport of
69 water vapor study with implication for global change, for example, what is the forcing
70 mechanism forming the vertical transport window of water vapor in the troposphere on the
71 TP? How is the AWT's special column constructor built for the vertical transport of
72 water vapor in the TP' troposphere? From the perspective of global atmospheric energy
73 and water vapor exchanges, this study characterizes a window of water vapor vertical
74 transport within the troposphere over the TP and the implication for global change.

75

76 **2. Data and Methods**

77 The daily meteorological data of cloud amount are provided by the meteorological
78 observatories in the TP in the period of 1979 to 2016. The AIRS remote sensing products
79 of water vapor and the ECMWF-interim data of meteorology are used in this study.



80

81 In this study, the inverse algorithm is used to calculate the apparent heat source Q_1 ,
82 and the formula is as follows(Su et al.,2006) :

$$83 \quad Q_1 = C_p \left[\frac{\partial T}{\partial t} + \vec{V} \cdot \nabla T + \left(\frac{p}{p_0} \right)^k \bar{\omega} \frac{\partial \theta}{\partial p} \right] \quad (1)$$

84 where T is air temperature; ω is the vertical velocity at the p coordinate, $P_0 = 1000$ hPa;
85 $k = R/C_p$; V is the horizontal wind vector; θ is the potential temperature.

86 Vertical integration of Q_1 is expressed as:

$$87 \quad \langle Q_1 \rangle = \frac{1}{g} \int_{p_t}^{p_s} Q_1 dp \quad (2)$$

88 where p_s is the surface air pressure, p_t is the top air pressure, here taken as 100hpa.

89

90 In order to analyze the relationship between water vapor source tracing and its
91 channels in the atmospheric water cycle over the TP, the correlation vector calculation
92 was used to calculate the temporal and spatial variations of the water vapor transport
93 channel. The expression is:

$$94 \quad \vec{R}(x, y) = R_u(x, y)i + R_v(x, y)j \quad (3)$$

95 where $\vec{R}(x, y)$ represents the correlation vector in which $R_u(x, y)$ represents the
96 correlation coefficients between rainstorm or precipitation frequency and the component
97 of latitudinal water vapor flux q_u , and $R_v(x, y)$ represents correlation coefficients
98 between rainstorm or precipitation frequency and longitudinal water vapor flux
99 components q_v .



100

101 **3. Results and discussion**

102 **3.1 The structures of vertical transport window of water vapor over the TP**

103 With the use of satellite remote sensing productions from 2003 to 2016, the global
104 distribution of the total water vapor from 500 hPa to 300hPa was calculated and shown in
105 Figures 1a . The results indicate that there is a high value center of the water vapor in the
106 mid- and upper troposphere over the TP, extending southwards to the Bay of Bengal,
107 India and Northern Southeast Asia. It is worth noting that the fraction of strong
108 convective cloud to the total cloud ranges from 4.0 % to 21.0 % in the TP, and the TP
109 during the summer season is dominated by the latent heat release (Fu et al.,2006; Dessler
110 et al.,2006; Gao et al.,2014). The intense mesoscale convective activity and the "massive
111 chimney effect" of huge cumulonimbus cloud continue to transport heat and water vapor
112 to the upper troposphere(Fu et al.,2006; Xie et al.,2018) . Based on Chinese Third
113 Tibetan Plateau Experiment-Observation of Boundary Layer and Troposphere (2014–
114 2017), it is observed that the mean cloud-top height was around 11.5 km (a.s.l.), and its
115 maximum value exceeded 19 km, and the mean cloud-base height was 6.88 km (a.s.l.)
116 during the observation period, reflecting the deep convection and its impact on the upper
117 troposphere.

118

119 **3.2 Global effect of the vertical transport window over the TP**

120 The vertical section of the correlation coefficients along the south-north direction
121 between the low cloud cover on TP and the global water vapor are presented in Figure 1b.
122 It could be noticed that there exists the structures similar with the massive chimney



123 between the convective cloud and the water vapor on TP (Figures 1b and 2a). It is
124 remarkable that the high correlation area exceeding the 95 % confidence level expand
125 towards the polar region of the southern and the northern hemisphere (Figure 1b), and the
126 relation between the convective clouds and the global water vapor in the upper
127 troposphere across the northern and southern hemispheres could be depicted.

128

129 The distributions of high positive correlation coefficients between low cloud
130 cover over the TP and the global the water vapor in the upper troposphere are calculated
131 by ECMWF-interim reanalysis data (Figure 3a). It can be found that there is a region with
132 highest values of correlation coefficients in the upper troposphere (500 hPa-300 hPa),
133 covering a banded area from the plateau to the lower latitude tropical zone to the polar
134 regions, which could indicate the significant correlations between convective cloud
135 activities on the TP and the global water vapor in the upper troposphere especially in the
136 polar region of the southern hemisphere area (Figure 3a).

137

138 The Indian continent heats up in spring and summer, convection draws moisture
139 northwards from the Bay of Bengal, Arabian Sea and Indian Ocean, leading to
140 precipitation in the Himalayas and beyond (Yanai et al., 1973). In Figure 3b, it could be
141 found that, driven by the strong apparent heat source, the warm and wet water vapor
142 flows on the Asian water tower (AWT) over the TP coming from the low latitude ocean
143 could build a remarkable channel. The key entrance to the water vapor passage is just the
144 intersection of the Himalayas on the southern slope of the TP. This region constitutes a
145 special canyon pass in the plateau with deep valleys, making a perfect entrance zone for



146 the oceanic warm-wet water flows (terrain in the lower right corner of Figure 3c).
147 According to the correlation analysis of water vapor transport, the water vapor source of
148 the AWT can also be traced back to the ocean surface water vapor source region with
149 water vapor positive correlation extreme value region in the Chagos archipelago of the
150 Central Indian Ocean near 10°S south of the equator (Figure 3d), revealing that the TP is
151 the confluence area of across hemispherical water vapor from the southern Indian Ocean.

152

153 **3.3 The transport window of water vapor driven by the AWT**

154 Through the correlation analysis of the whole layer of apparent heat source Q_1 over
155 the plateau region, the three-dimensional structure of vorticity and divergence, it can be
156 found that the apparent heat source Q_1 in TP are an important forcing factor (Figure 4).
157 The results show that the air heat island over the AWT is located at 300-500 hPa (Figure
158 5). The Q_1 is significantly related to the convective cloud and its strong ascending
159 movement (Figures 3b-3d), and there exists also a strong high-level anticyclone in the
160 region of the AWT in the southeast of the plateau (Figure 3d). In addition, the lower
161 troposphere is the center of strong convergence and strong vorticity (Figure 4). All these
162 results reveal the effective "pumping effect" of the vertical configuration with low-level
163 cyclonic circulation and high-level divergence with anticyclone circulation in TP (Figures
164 3b-3d). The strong confluence effect could be driven by the elevated heating on the TP
165 in the middle troposphere with the water vapor flow, making a strong warm wet vapor
166 transport channel connecting the water vapor source in the low latitude tropical ocean
167 with the water vapor center over the core area of AWT.

168



169 **4. Conclusion**

170 By using the multi-source data of meteorology over recent decades, this study
171 discovered a summertime “hollow wet pool” in the troposphere with a center of high
172 water vapor over AWT on the highly elevated TP, where is featured by a vertical
173 transport window with the transport flux columns of water vapor in the troposphere.
174 Driven by the strong TP’s heat source, water vapor flows are connected the AWT over
175 the TP with the low-latitude oceans. Significant correlations exist between convective
176 activity on the TP and water vapor in the upper-troposphere especially in the polar region
177 of the southern hemisphere. The water vapor transport from the TP’s vertical window in
178 the upper troposphere extends globally towards the northern and southern hemispheres
179 from the TP with the significant connections among the three poles of Arctic, Antarctic
180 and TP regions, highlighting an effect of TP’s vertical transport window of water vapor
181 on global change. The vertical transport window was built by the AWT’s thermal forcing
182 in associated with the dynamic effect of the TP’s “hollow heat island” as well as the
183 effective "pumping effect" of low-level convergence with cyclonic circulation and high-
184 level divergence with anticyclone circulation over the TP.

185 In this observational study, a conceptual model of the comprehensive relation of the
186 TP region with the global energy and water cycles under the thermal forcing in the core
187 region of the AWT was put forward for the vertical transport window of vapor (Figure 6),
188 where the "core area" of AWT is the key entrance of the low-latitude warm and moist air,
189 and the water vapor source was traced back to the Southern Hemisphere. The heat driving
190 effect on the TP could contribute to the maintenance of vertical upward transport of the
191 energy and water vapor. The water cycle in the AWT clearly displayed the connection



192 with the warm-wet vapor source in the tropical oceans and the southern Indian Ocean.
193 Our study depicted a comprehensive understanding on the vertical water vapor transport
194 in the atmosphere over the TP with an important implication to global change.

195

196 ***Data availability***

197 ERA-Interim (

198 ECMWF, <https://apps.ecmwf.int/datasets/data/interim-full-mods/levtype=pl/>) reanalysis

199 daily and monthly data are part of the European Center for Medium-range Weather

200 Forecasts. AIRS Science Team/Joao Teixeira (2013), AIRS/Aqua L3 Daily Standard

201 Physical Retrieval (AIRS-only) 1 degree x 1 degree V006, Greenbelt, MD, USA,

202 Goddard Earth Sciences Data and Information Services Center (GES DISC),

203 Accessed: [Jan. 2019], 10.5067/Aqua/AIRS/DATA303. The low cloud data used in this

204 study are derived from the Data Sets of Surface Meteorological Elements in China

205 released by the National Meteorology Information Center, China Meteorological

206 Administration, which can be found at

207 <https://zenodo.org/record/5121157#.YPkRHqjitPY>

208 (<http://doi.org/10.5281/zenodo.5121157>).

209

210 **Author Contributions**

211 Xiangde Xu, Chan Sun and Tianliang Zhao conducted the study design. Deliang Chen,

212 Jianjun Xu and Shengjun Zhang analysed the observational data. Juan Li, Bin Chen,



213 Yang Zhao, Lili Dong, Xiaoyun Sun, and Yan Zhu assisted with data processing.
214 Xiangde Xu and Tianliang Zhao wrote the manuscript. Xiangde Xu, Chan Sun, Tianliang
215 Zhao, and Jianjun Xu were involved in the scientific interpretation and discussion. All
216 authors provided commentary on the paper.

217

218 **Acknowledgments**

219 This study was supported by The Second Tibetan Plateau Scientific Expedition and
220 Research (STEP) program (2019QZKK0105) and the Scientific and Technological
221 Development Funds from Chinese Academy of Meteorological Sciences (2021KJ022 and
222 2021KJ013).

223

224 **Financial support.**

225 This study was supported by The Second Tibetan Plateau Scientific Expedition and
226 Research (STEP) program (2019QZKK0105) and the Scientific and Technological
227 Development Funds from Chinese Academy of Meteorological Sciences (2021KJ022 and
228 2021KJ013).

229

230 **Conflict of interest**

231 *Xiangde Xu, Chan Sun, Deliang Chen, Tianliang Zhao, Jianjun Xu, Shengjun Zhang,*
232 *Juan Li, Bin Chen, Yang Zhao, and Lili Dong declare that they have no conflict of*
233 *interest.*

234



235

236 **References**

237 Chen, B., Xu, X. D., Yang, S., and Zhao, T. L.(2012). Climatological perspectives of air transport from
238 atmospheric boundary layer to tropopause layer over Asian monsoon regions during boreal summer
239 inferred from Lagrangian approach. *Atmos. Chem. Phys.* ; 12: 5827-5839. [https://doi.org/10.5194/acp-](https://doi.org/10.5194/acp-12-5827-2012)
240 12-5827-2012

241 Dessler, A and Sherwood, S. (2004). Effect of convection on the summertime extratropical lower
242 stratosphere. *J. Geophys. Res.* 109: D23301. <https://doi.org/10.1029/2004JD005209>

243 Feng, L., and Zhou, T. (2012).Water vapor transport for summer precipitation over the Tibetan Plateau:
244 Multidata set analysis, *J. Geophys. Res.*, 117, D20114, doi:10.1029/2011JD017012

245 Fu, R., Hu, Y., Wright, J., Jiang,J., H., Dickinson, R., E., Chen, M., X., Filipiak, M., Read, W., G., Waters,
246 W., W.,and Wu, D., L. (2006). Short circuit of water vapor and polluted air to the global stratosphere
247 by convective transport over the Tibetan Plateau, *Proceedings of the National Academy of Sciences of*
248 *the United States of America.* 103: 5664-5669. <https://doi.org/10.1073/pnas.0601584103>

249 Gao, Y, Cuo, L and Zhang, Y. (2014).Changes in Moisture Flux over the Tibetan Plateau during 1979–
250 2011 and Possible Mechanisms. *J. Climate* ; 27: 1876-1893.[https://doi.org/10.1175/JCLI-D-13-](https://doi.org/10.1175/JCLI-D-13-00321.1)
251 00321.1

252 Garny, H. and Randel, W. J. Transport pathways from the Asian monsoon anticyclone to the stratosphere,
253 *Atmos. Chem. Phys.* (2016); 16: 2703–2718, [https://doi.org/10.5194/acp-16-2703-](https://doi.org/10.5194/acp-16-2703-2016) 2016,.

254 James, R. , Bonazzola, M. , Legras, B. , Surbled, K. , & Fueglistaler, S. . (2008).Water vapor transport and
255 dehydration above convective outflow during Asian monsoon. *Geophys. Res. Lett.* ; 35: L20810.
256 <https://doi.org/10.1029/2008GL035441>

257 Luo, Y. , Zhang, R. , Qian, W. , Luo, Z. , and Hu, X. . (2011). Intercomparison of deep convection over the
258 tibetan plateau--asian monsoon region and subtropical north america in boreal summer using
259 cloudsat/calipso data. *Journal of Climate.* 24: 2164-2177.



- 260 Randel, W. J. & Jensen, E. J. (2013). Physical processes in the tropical tropopause layer and their roles in a
261 changing climate. *Nat. Geosci.*, 6, 169. <https://doi.org/10.1038/ngeo1733>
- 262 Solomon, S., Rosenlof, K. H., Portmann, R. W., Daniel, J. S., Davis, S. M., Sanford, T. J. and Plattner,
263 G. K. (2010). Contributions of stratospheric water vapor to decadal changes in the rate of global
264 warming. *Science*, 327: 1219–1223. <https://doi.org/10.1126/science.1182488>
- 265 Su, H, Read, W, Jiang, J. H. , Waters, J. W. , and Fetzer, E. J. . (2006). Enhanced positive water vapor
266 feedback associated with tropical deep convection: New evidence from Aura MLS. *Geophys. Res.*
267 *Lett.* ; 33. <https://doi.org/10.1029/2005GL025505>
- 268 Tian, B, Soden, B, Wu, X. (2004). Diurnal cycle of convection, clouds, and water vapor in the tropical
269 upper troposphere: Satellites versus a general circulation model. *J. Geophys. Res. Atmos.*; 27: 2173–
270 2176. <https://doi.org/10.1029/2003JD004117>
- 271 Tian, W. S., Chipperfield, M. and Lü, D. R. (2009). Impact of increasing stratospheric water vapor on
272 ozone depletion and temperature change. *Adv. Atmos. Sci.* ; 26: 423–
273 437. <https://doi.org/10.1007/s00376-009-0423-3>
- 274 Wang, Y, Zhang, Y, Chiew, F., McVicar, T., R., Zhang, L., Li, H., and Qin, G. (2017). Contrasting
275 runoff trends between dry and wet parts of eastern Tibetan Plateau, *Sci. Rep. U.K.* 7: 15458.
276 <https://doi.org/10.1038/s41598-017-15678-x>
- 277 Xie, F., Zhou, X., Li, J., Chen, Q., Zhang, J., Li, Y., Ding, R., Xue, J. and Ma, X. (2018). Effect of the
278 Indo-Pacific Warm Pool on lower stratospheric water vapor and comparison with the effect of the El
279 Niño–Southern Oscillation. *J. Clim.* 31:929–943.
- 280 Xu, K., Zhong, L., Ma, Y., Zou, M., and Huang Z., (2020). A study on the water vapor transport trend and
281 water vapor source of the Tibetan Plateau. *Theor. Appl. Climatol.*, **140**, 1031–1042,
282 <https://doi.org/10.1007/s00704-020-03142-2>.

283



- 284 Xu, X, Zhao, T, Lu C., Guo, Y., Chen, B., Liu, R., Li, Y., and Shi, X. (2014). An important mechanism
285 sustaining the atmospheric "water tower" over the Tibetan Plateau. *Atmos. Chem. Phys.* 14: 11287-
286 11295. <https://doi.org/10.5194/acp-14-11287-2014>
- 287 Xu, X., Lu, C. Shi, X. and Gao, S. (2008). World water tower: An atmospheric perspective, *Geophys. Res.*
288 *Lett.*, 35, L20815. <https://doi.org/10.1029/2008GL035867>
- 289 Yanai, M. , Esbensen, S. , and Chu, J. H. . (1973). Determination of bulk properties of tropical cloud
290 clusters from large-scale heat and moisture budgets. *Journal of Atmospheric Sciences*, 30(4), 611-
291 627. [https://doi.org/10.1175/1520-0469\(1973\)030<0611:DOBPOT>2.0.CO;2](https://doi.org/10.1175/1520-0469(1973)030<0611:DOBPOT>2.0.CO;2)
- 292



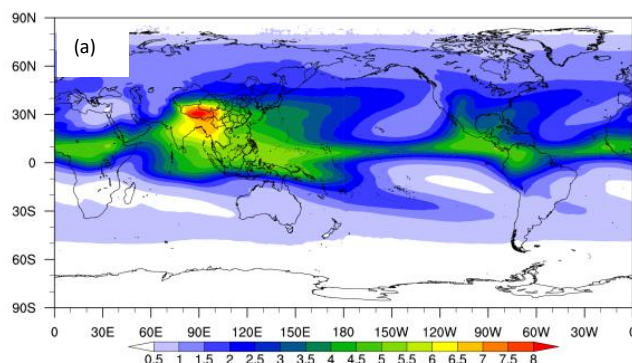
293

294

295

296

297

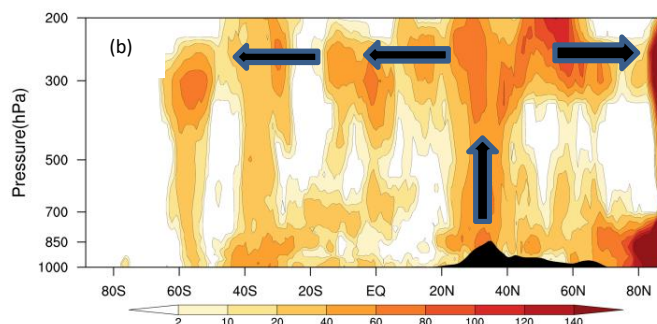


298

299

300

301



302

303 **Figure 1.**(a) the global distribution of the total water vapor from 300 hPa to 500 hPa
304 based on the summertime AIRS data from 2003 to 2018, (b) the vertical section of the
305 frequency (shaded) of the correlation coefficients passing the level of 90%
306 confidence between summertime TP's low cloud cover and the water vapor at different
307 vertical levels along the meridional direction averaged over 60oE - 180oE for 1979-
308 2016 with the black arrows indicating the connections of TP's low clouds to global water
309 vapor in the upper troposphere with high frequencies.

310

311

312



313

314

315

316

317

318

319

320

321

322

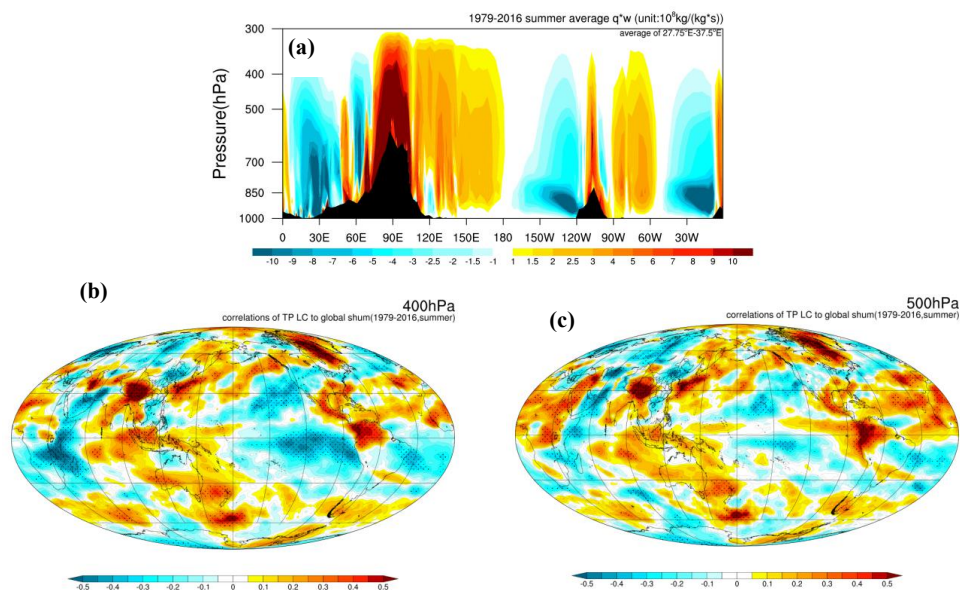
323

324

325

326

327



328

329

330

331

332

333

334

335

336

337

338

339

340

Figure 2 (a) Vertical section of vertical vapor transport flux averaged over 27.5-32.0°N in summers of 1979-2016; the spatial distributions of lag correlation coefficients of low cloud cover over the TP during May, June and July with the global specific humidity of the ECMWF-interim data in Summer from 1979 to 2018 at (b) 400 hPa and (c) 500 hPa.



341

342

343

344

345

346

347

348

349

350

351

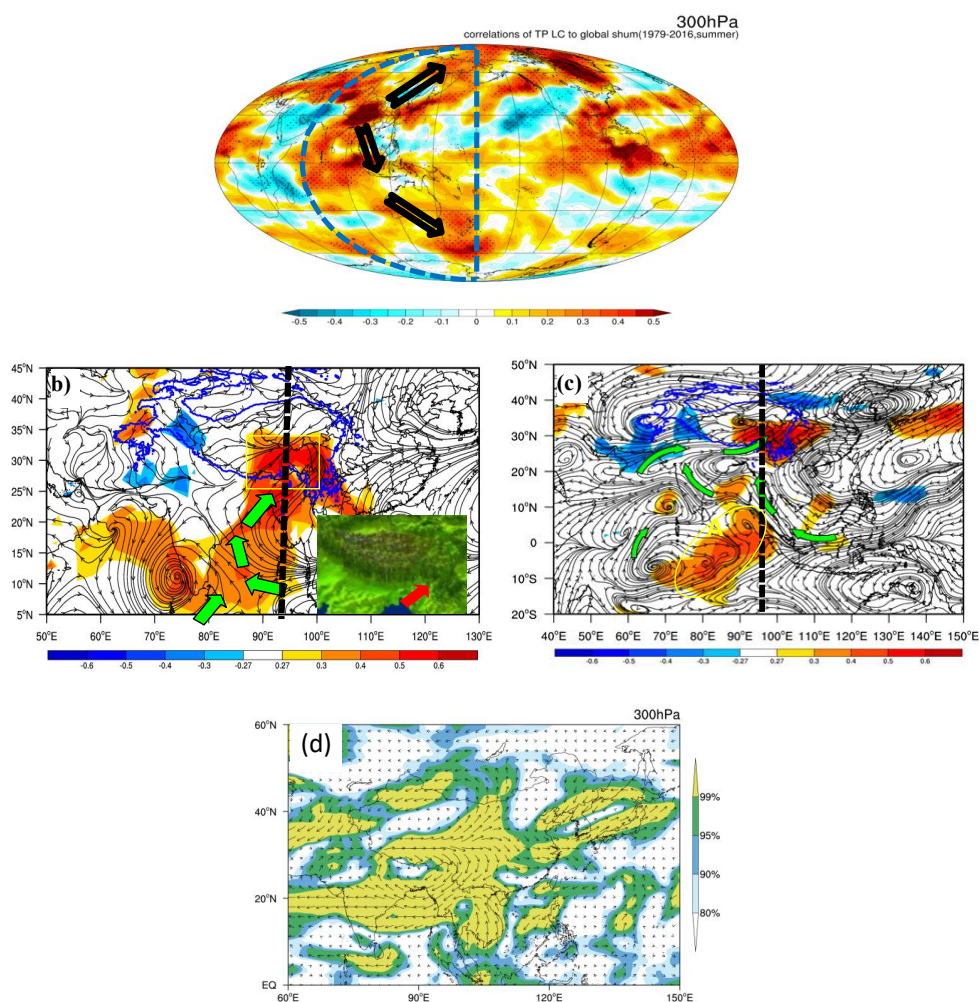
352

353

354

355

356



357

358

359

360

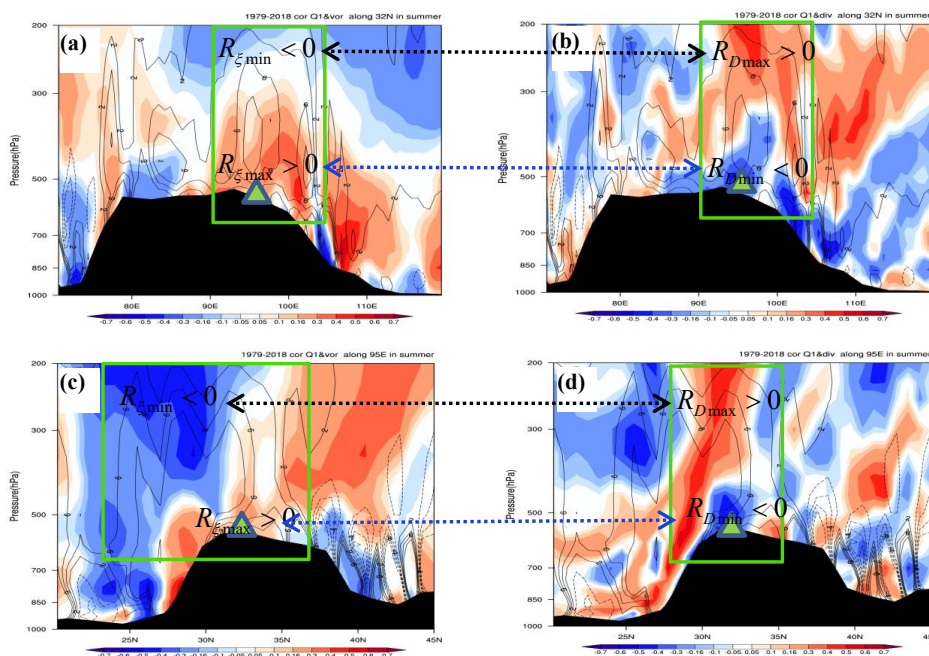
361

362

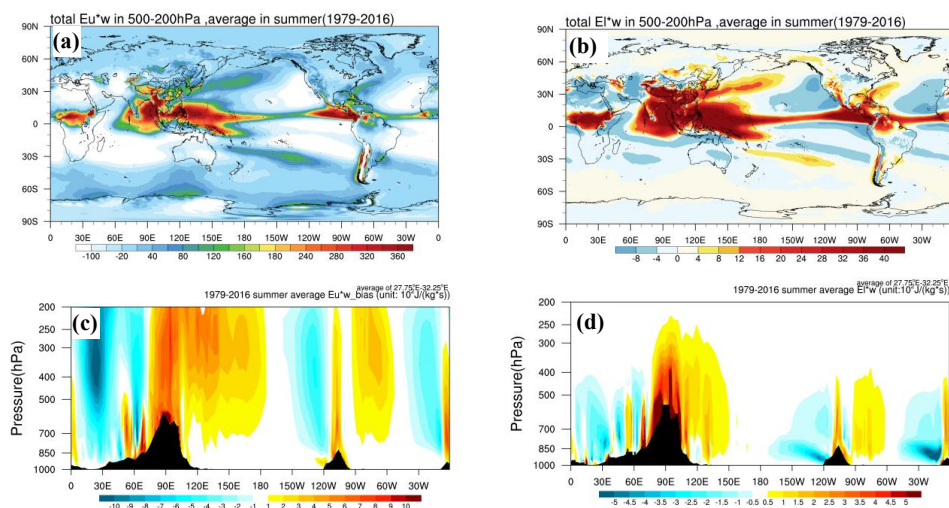
Figure 3. (a) The spatial distributions of correlation coefficients of low cloud cover over the TP with the global specific humidity of the ECMWF-interim data at 300 hPa in summers of 1979-2016 with the pathways of convective air to the troposphere, (b) the fields of correlation vectors (stream lines) of the TP-column Q_1 integrated over the TP region (80-102°E; 30-37.5°N) with the water vapor fluxes near the surface layer (the yellow rectangle frame denoting the AWT), (c) the water vapor fluxes at 500 hPa, (d)



363 correlation vectors of TP-column Q1 integrated over the TP region (80-102°E; 30-37.5°N)
364 to 300hPa vapor transport flux in July 2014-2016.
365



366
367 **Figure 4.** The vertical sections of (a) vertical motion (contours, in unit: $10^{-2} \text{ Pa}\cdot\text{s}^{-1}$) and (c)
368 correlation coefficients (shaded) between Q_1 and the vorticity as well as the correlation
369 coefficients between Q_1 and the divergence (b, d) separately in the core region of the
370 AWT, in which, a, b is along 32°N , and c, d is along 95°E . The green triangle is the
371 AWT.
372



373

374 **Figure 5.** The summertime average distribution of (a) the total inner energy and (b)
375 latent heat energy, as well as the vertical profiles of (c) the inner energy and (d) latent
376 heat energy transporting upward from 1979 to 2017 along the east-west direction
377 (27.5°N-32.0°N) over the TP.

378

379

380

381

382

383

384

385

386

387

388



389

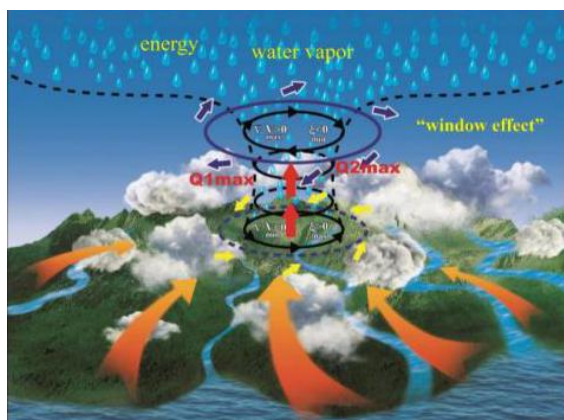
390

391

392

393

394



395 **Figure 6.** a diagram of water vapor transport to the troposphere driven by the thermal
396 forcing of AWT over the TP.

397

398

399

400

401

402

403

404

405

406

407

408